NRC Research Press

ARTICLE

Clear wood content in standing trees predicted from branch scar measurements with terrestrial LiDAR and verified with X-ray computed tomography[1]

Stefan M. Stängle, Franka Brüchert, Ursula Kretschmer, Heinrich Spiecker, and Udo H. Sauter

Abstract: Knowledge about the wood quality of standing trees is crucial in that it serves as an excellent means for nearly all stages of the wood-supply chain. Better information about internal wood characteristics can be derived from the outside appearance by establishing a correlation between the bark characteristics of a stem and its internal quality. This paper presents an approach where the quality determination of standing trees using a terrestrial light detection and ranging (LiDAR) system is combined with the information about internal quality of logs using X-ray computed tomography (CT). Results show a high accuracy for branch scar measurements with terrestrial LiDAR and knot measurement with CT. A strong correlation between scar seal quotient and the amount of clear wood could be confirmed using European beech (*Fagus sylvatica* L.) as an example. Quality grading of virtually segmented logs using terrestrial LiDAR and CT showed moderate correlation; 62.5% of the segments were allocated to the same grade by both approaches. In conclusion, terrestrial LiDAR in forest inventory could be used as an instrument to predict inner wood quality in greater detail by gathering data on the outer appearance and branch scars of standing trees. This additional knowledge has the potential to improve forest planning, bucking instructions, and a roundwood allocation that meets industry demand.

Résumé : Il est essentiel de connaître la qualité du bois des arbres sur pied car cela est d'une grande utilité à presque toutes les étapes de la chaîne d'approvisionnement en bois. Une meilleure information au sujet des caractéristiques internes du bois peut être dérivée de l'apparence externe en établissant une corrélation entre les caractéristiques de l'écorce d'une tige et sa qualité interne. Cet article présente une approche qui consiste à déterminer la qualité des arbres sur pied à l'aide d'un système lidar terrestre (détection et télémétrie par la lumière) combiné à des informations sur la qualité interne des billes obtenues grâce à la tomodensitométrie aux rayons X (CT). Les résultats montrent la grande précision des mesures de cicatrice de branche avec le lidar terrestre et de celles des nœuds avec le CT. Une étroite corrélation entre le rapport hauteur/largeur des cicatrices de branche et la quantité de bois sain a pu être confirmée en utilisant le hêtre commun (*Fagus sylvatica* L.) comme exemple. Les classements par qualités des billes virtuellement segmentées à l'aide du lidar terrestre et du CT étaient modérément corrélés : 62,5 % des segments ont été attribués à la même classe par les deux approches. En conclusion, le lidar terrestre pourrait être utilisé dans les inventaires forestiers pour prédire la qualité interne du bois de façon plus détaillée en récoltant des données sur l'apparence externe et les cicatrices de branche des arbres sur pied. Cette information additionnelle pourrait améliorer la planification forestière, les instructions de tronçonnage et l'allocation des bois ronds en fonction des spécifications de l'industrie. [Traduit par la Rédaction]

Introduction

One major quality feature of sawlogs is the ratio between knotty core and clear wood. After trees are naturally or artificially pruned, knots become occluded and clear wood is formed around the knotty core. In general, clear wood yields sawn timber of higher grade and is, therefore, more valuable. The occurrence of knots has been described as one of the most significant defects affecting the yield from hardwood sawlogs in the early 20th century (Mayer-Wegelin 1936). Up to today, the amount and the size of visible knots on board surfaces are important grading features and strongly influence timber prices, especially for hardwood species such as European beech (*Fagus sylvatica* L.) and oak (*Quercus petraea* (Matt.) Liebl. and *Quercus robur* L.). Even a single knot can downgrade sawn timber and substantially reduce the value (DIN Standard 2011). Artificial pruning to increase the clear wood content and, therefore, roundwood quality has been a silvicultural

treatment for a very long time for softwoods and also for hardwoods (Mayer-Wegelin 1936; Curtis 1937; O'Hara 1989, 2007; Nicolescu 1999; Hein and Spiecker 2007). Because of substantial price differences for wood of different quality grades, estimates on the amount of clear wood in standing trees are crucial for the estimation of the value of a forest. The dimension and the shape of the knotty core differ between trees of different age, diameter, genetics, site conditions, and silvicultural treatment (Storch 2011).

The precise quality of timber is not known prior to sawing the wood and can only be estimated by external wood characteristics. Different approaches exist to predict wood properties of trees and sawlogs. On a stand basis, growth models can be applied (e.g., Mäkinen and Song 2002; Moberg and Nordmark 2006). Other approaches attempt to predict wood properties from external tree characteristics of single trees (e.g., Wernsdörfer et al. 2006). For trees from homogeneous stands such as artificially pruned coniferous plantations, indexes have been developed to predict the

Table 1. Parameter descriptions for the four study sites.

	Study site			
	1	2	3	4
Forestry administration unit, District/Stand	Emmendingen, Tennenbach/ Prängewald	Emmendingen, Kandelwald/ Eckschlag	Karlsruhe, Zehntwald/ Oberer Kartoffelschlag	Karlsruhe, Südl. Wildpark/ Zwei-Eichen-Schlag
Coordinates (Gauss-Krüger, zone 3)	3417800, 5335700	3428000, 5326700	3457000, 5435800	3458200, 5434700
No. of trees felled	4	10	8	11
No. of trees scanned with t-LiDAR	4	0	8	6
Tree age (years), range and mean	38–110/60	81–161/131	101–120/110	121–140/130
Area (ha)	8.5	12.9	13.6	6.8
Terrain	370 m a.s.l., moderately steep	1030 m a.s.l., steep	110 m a.s.l., flat	110 m a.s.l., flat
Exposure	NNW	SW	—	—
Mean annual air temperature (°C)	9.1	5.9	10.2	10.2
Annual precipitation (mm)	1075	1770	760	770
Tree species (share in %)	*Fagus sylvatica* (65), *Larix decidua* (15), other (20)	*Fagus sylvatica* (70), *Picea abies* (30)	*Pinus sylvestris* (60), *Fagus sylvatica* (40)	*Pinus sylvestris* (80), *Fagus sylvatica* (20)

Note: t-LiDAR, terrestrial LiDAR.

clear wood potential with easy to measure log variables (e.g., Park 1989). The availability of such information from inventory plots allows stand-based modeling for quality and value calculation and prediction of stand development.

Alternatively, noninvasive technologies such as X-ray computed tomography (CT) can be used to assess the actual clear wood content of each sawlog in the processing chain of a sawmill. CT technology has proven to be useful for the assessment of internal wood features, especially the size and position of knots. An overview of CT application in wood quality assessment is given by Wei et al. (2011).

Despite the high interest in clear wood prediction and the efforts made to develop suitable methods, usually the seller or buyer do not have exact information about internal knots and the amount of clear wood when trading roundwood. Knoke et al. (2006) identified the current five most important quality indicators for buyers of beech logs: red heartwood, spiral grain, stem curvature, roughness of the bark, and growth stresses. None of these criteria, however, influences the potential sawn timber value as much as the amount of clear wood.

For many tree species with a smooth bark surface, the size and position of internal knots and, therefore, the amount of clear wood, can be estimated by considering the branch scar geometry. The scar seal can be assumed to be circular when a branch stump or a dead branch is becoming overgrown. With increasing diameter of the tree at continuing growth in girth, the width of the seal is stretched, whereas the height stays constant. Schulz (1961) showed that the ratio between the height and width of a scar seal, also known as scar seal quotient, is directly related to the size of the subjacent knot for European beech. Strong correlations between the shape of scar seals and internal defects have also been confirmed for other hardwood species (Thomas 2009). Current German grading standards for roundwood (DIN Standard 2013; Anonymous 2012) consider the seal quotient of covered knots as grading criterion.

Terrestrial light detection and ranging (LiDAR) is a technology that can be used for detailed forest inventory and the digital reproduction of tree characteristics at high resolution (Dassot et al. 2011). Schütt et al. (2004) showed that the assessment of branch scars is possible with terrestrial LiDAR (t-LiDAR). This approach was used by Van Goethem et al. (2008) to connect exterior bark characteristics to internal knots. For implementation in practice,

however, automation of the detection process is essential. An automated approach for detecting surface defects in sawmills was developed by Thomas and Thomas (2011).

If t-LiDAR works as a tool for scar seal measurements, this technology could be used to assess the amount of clear wood for standing trees of a species, for which the correlation between scar seal quotient and the amount of clear wood is valid.

The correlation between scar seal quotient and the size of branch occlusion mostly has been tested destructively (Schulz 1961; Hein 2008; Thomas 2009). One established method to measure the size of overgrown knots is to cut in a line from the center of a scar seal to the pith and measure knot parameters on the cut surface (Hein and Spiecker 2007). This method, however, is time consuming and is limited to knots that show an obvious branch scar. With this approach, it is not possible to detect knots that were overgrown long ago and it is also problematic when analyzing small knots. The shortcomings of this method could be overcome by using the nondestructive technology of X-ray CT. With this method, X-rays are internally reflected and partially absorbed to different degrees by wood of different densities. As a result, internal wood features such as tree rings, knots, and rot can be detected on CT images. CT has been shown to be suitable for the assessment of internal wood features, such as knots, in detail (Wei et al. 2011).

The objective of this study was to test t-LiDAR as a tool for clear wood prediction of standing trees by applying the branch seal quotient.

First, the accuracy of knot measurements with CT and branch scar measurements with t-LiDAR was assessed. Secondly, the correlation between scar seal quotient and the size of branch occlusion for European beech was validated, and, finally, predictions of clear wood based on branch scar measurements were compared with results from the CT analysis.

Material and methods

Study objects

The 33 trees selected for this study were sampled from four mixed-species stands in Baden-Württemberg, South West Germany (Table 1). The stands had mean ages between 60 and 130 years and covered a wide range of mean annual air temperatures and

Table 2. Quality grades of the studied logs.

	Quality grade					
	A	B	C	D	NA	Sum
All logs	2	19	33	29	2	85
Subset	2	18	25	19	—	64

Note: Grading according to EN 1316-1:2012 (DIN Standard 2013).

Fig. 1. 2D images of the point clouds from two of four performed scans of one exemplary tree. Grayscale represents the reflectance value. Background of surrounding trees and other vegetation was removed by automated filtering and manual postprocessing.

precipitation. The trees had different numbers of branches and of overgrown knots, which also differed in size. While still standing in the forest, the trees were labeled for unique identification and tree height (dm) and diameter at breast height (DBH; mm) were recorded.

For the t-LiDAR measurements, a subset of 18 trees showing DBHs between 35 and 45 cm was selected within study sites 1, 3, and 4. To allow tree identification in the laser-scanned images, the trees were clearly marked by scratching the bark at several positions. After scanning the subset, all 33 trees were felled and bucked to 85 logs of approximately 4 m in length and then transported to the Forest Research Institute of Baden-Württemberg (FVA) in Freiburg for further analysis.

All 85 logs were graded according to the quality grading standards of EN 1316-1:2012 (DIN Standard 2013) by visually evaluating 3D reconstructions from CT recordings. According to these standards, the outer appearance of a stem or log is graded by a descriptive analysis of shape, crook, spiral growth, cracks, the number and size of branches or the occurrence of branch scars, and other defects. The categories A to D describe four grades of decreasing quality, where grade A must not show any devaluating features. CT scanning was performed on all 85 logs, however, a detailed analysis could not be performed for all of them. Thus, only a subset of 64 logs was used for the data analysis. The logs that were selected for further analysis were, on average, of higher quality than the average harvested log (Table 2).
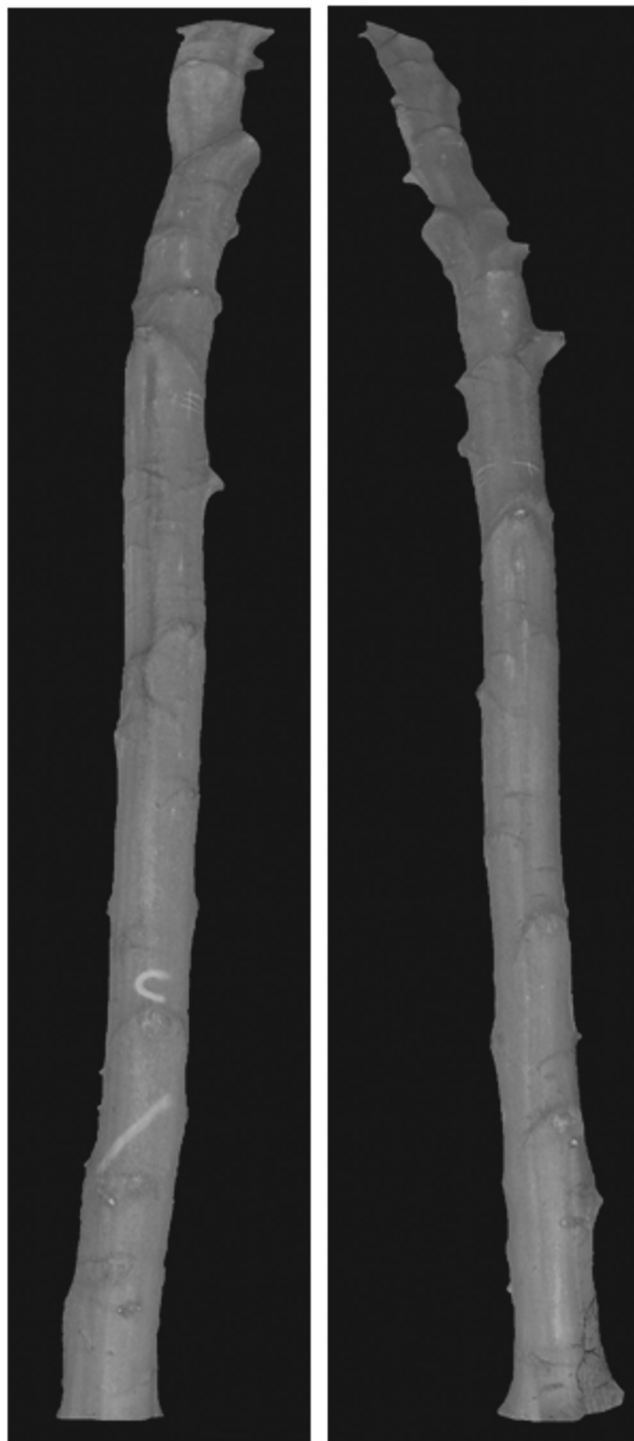
Branch scar assessment

t-LiDAR

Eighteen trees were scanned by a Zoller+Fröhlich Imager 5006 from four different positions to assess the entire surfaces of the tree stems. The trees of study site 1 were scanned with a resolution of 20 000 pixels / 360° in horizontal and vertical directions, and the trees of study sites 3 and 4 were scanned with a resolution of 10 000 pixels / 360° in both directions. Resolution was changed to test whether bark features can be recognized easier at a higher resolution. The closer an object is to a laser scanner, the higher the data point density on the object's surface. The average distance from the laser scanner to the trees was 4.1 m. Recorded data points at the height of the scanner (1.5 m above ground) were 1.1 and 2.2 mm away, respectively, from each other in the two chosen resolutions. Strictly following trigonometric functions, at a tree height of 12.5 m, the distances between the data points were 3.1 and 6.2 mm. The exact x,y,z coordinates and the intensities of reflectance for all points that were reached by laser beams were recorded by the 3D laser scanner. In Fig. 1, intensity values of two scans of the stem of one isolated tree are shown. This information is very similar to the one in a grayscale photo. The analysis of the t-LiDAR data was limited to the measurement of branch scars, as these are the most important quality-indicating feature on branch-free stems. Height and width of 42 scar seals (mm) were measured either by the use of the intensity data or by the use of a bark surface model.

Laser beams are reflected in a different intensity by branch scars than by the surrounding smooth bark. Zoller+Fröhlich LaserControl 3D analysis software (version 8.1.0) was used to identify all branch scars that were visible in the intensity data (Fig. 2). For this analysis, the scanner position matches the origin of the data points and no coordinate transformation is required. This method

was sufficient for the identification and measurement of most of the scars. The analysis of the intensity data, however, did not allow the detection of all existing branch scars, so a more sophisticated approach to assess the scars was tested. To generate a more accurate reconstruction of the bark surface, each tree stem was modeled by a series of consecutive cylinders using the algorithms described by Pfeifer and Winterhalder (2004). The cylinder length

Fig. 2. Labelled bark scar on a stem in color (left) and the same scar in the intensity image of the terrestrial LiDAR data (right).
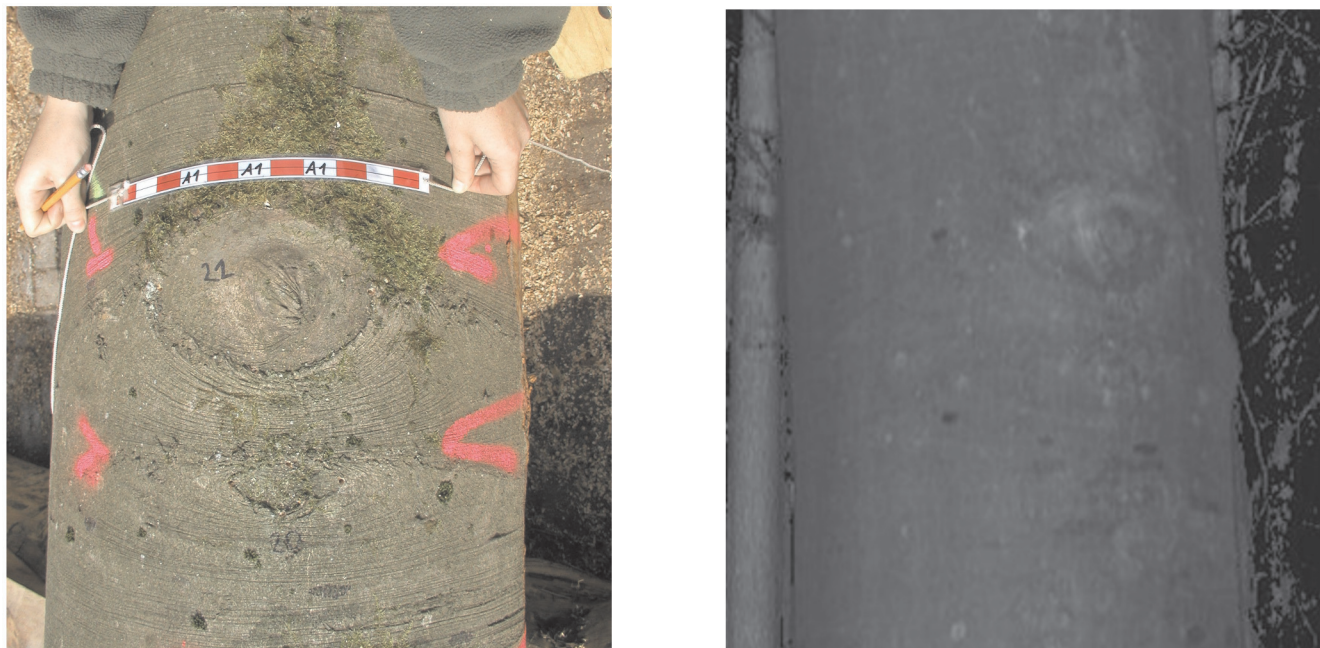
was automatically chosen to best represent the form of the tree stem with respect to taper and sweep. This procedure resulted in a mean cylinder length of 12.2 cm and a maximum length of 16.7 cm. The surface of these cylinders was projected on a flat surface (Schütt et al. 2004). All stem points were then displayed in relation to this surface to create a bark surface model (Fig. 3). All radial deviation in the tree from the cylindrical approximation (such as branch scars) was, therefore, displayed as heights above the flat surface. This was realized by use of the numerical computing environment MATLAB (R2011b). The advantage of the bark surface model is a better visibility of small deviations from the relatively flat surface, which allows more accurate measurements of branch scars that did not show much difference under laser reflectance compared with the surrounding bark. The change of the coordinate system allows the focus to be on radial deviations and enables the detection and measurement of scars protruding above the bark surface.

Reference measurements

Position and size of all branch scars that were visible on the bark surface were manually assessed on all 85 logs. For each branch scar, the height and width of the scar seal (mm) and the height of the Chinese moustache (mm) were measured (Fig. 4 left). Each scar position was described by its distance from the log end (z position) and the distance on the log surface from a color-marked reference line. This distance was used to calculate the azimuth from the reference line. This data was used to validate the accuracy of t-LiDAR scar measurements and to test for the relation between external features and internal wood defects.

Knot measurements

CT

All logs were scanned with the CT.LOG (MiCROTEC, Italy) located at the Forest Research Institute in Freiburg. For the scans, a voltage of 180 kV, a current of 14 mA, and 900 views per rotation were used. The resolutions were 1.1 and 5 mm for the radial and longitudinal directions, respectively. From the raw data, a three-dimensional data block was computed where the grayscale value of each voxel (3D pixel) represented the density (kg·m⁻³) as calcu-

lated from the amount of X-ray absorption and X-ray scattering of the corresponding point in the log.

The first step of the analysis of the CT images was an automated detection of the pith using a modification of the algorithm described by Longuetaud et al. (2004) in proprietary software developed by the Forestry Research Institute and MiCROTEC. Being the origin of all knots, the position of the pith is important for the analysis of knot sizes in CT data. In the next step, the images were manually examined for knots, which could be identified as the grayscale values in the knots contrasted with those in the surrounding wood. For every clearly visible knot, the radial distance from the pith to the end of the sound part, to the end of the dead part, and the height and width of the knot at every 20 mm step from the pith were recorded (mm) (Fig. 5). The position of the starting point for each knot was described by its x,y,z coordinates in the log. The growth direction of the knots was described by the azimuth to a reference line, which was marked with metal nails for visibility in the CT images. Knots originating from epicormic shoots, which were found in some of the logs, were not assessed as a close relation between scar seal quotient and clear wood content cannot be expected for this type of knot. Epicormic shoots originate from epicormic buds and are produced after the stress exposure of a tree (Colin et al. 2008). Therefore, the starting point of epicormic knots is not in the pith but somewhere between pith and bark. Without knowing the knot origin, eq. (1) cannot be applied to calculate the clear wood content.

Manual reference measurements

Twenty-six knots of lengths ranging from 20 to 170 mm were selected from the CT images for manual validation measurements. These particular sections of the logs were cut longitudinally in a line from the center of the corresponding branch scar seal to the pith to measure the largest extent of the knot in the radial and longitudinal directions.

Amount of clear wood

Measured parameters of the branch scars and the knots are displayed in Fig. 4. Height (h) and width (w) are measured as straight lines between the edges of the seal. The height of the

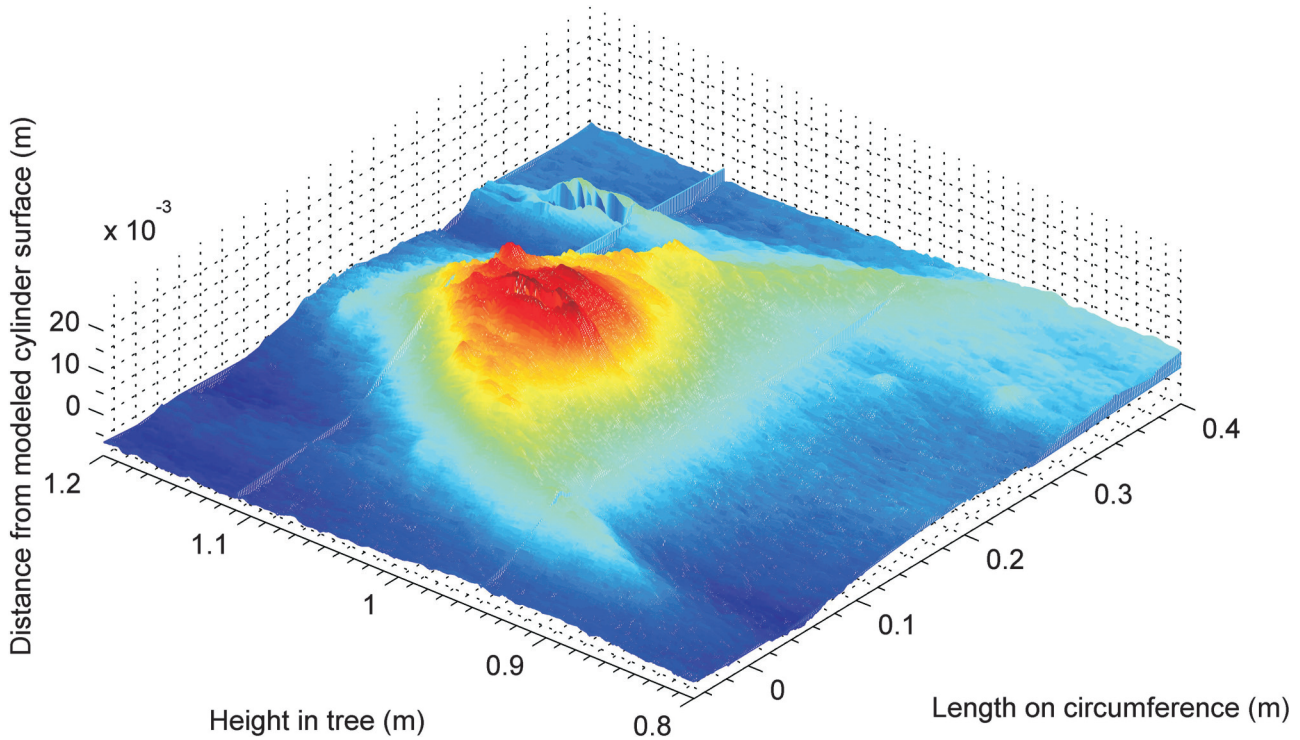**Fig. 3.** Bark surface model of a branch scar generated from terrestrial LiDAR data.

Fig. 4. Branch scar consisting of the scar seal described by scar seal width (w) and height (h) and the Chinese moustache described by height (h_m) (left). Longitudinal cut revealing the maximum knot diameter (d), the knot height (h_k) the radius at time of knot occlusion (r_1), and the current radius (r_2) (right). (Adapted from Schulz (1961) and Knigge and Schulz (1966)).
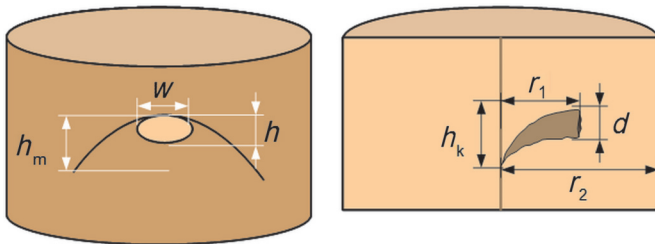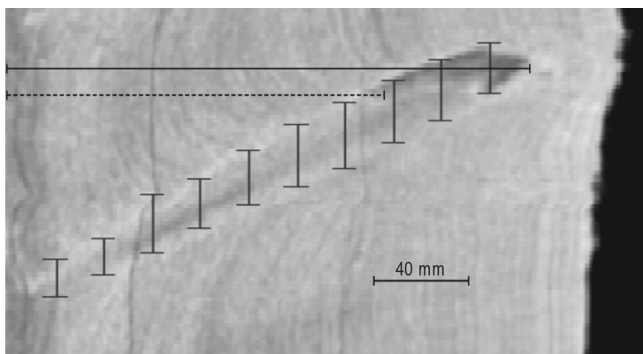

Fig. 5. Computed tomography (CT) image of a knot. Vertical lines represent the diameter of the knot at every 20 mm step. The broken line represents the length of the sound part of the knot and the solid line represents the total knot length including the dead part.

Chinese moustache (h_m) can be assumed to reflect the knot height (h_k), which is defined as the vertical distance between the knot origin in the pith and the upper edge of the branch seal (Knigge and Schulz 1966). The maximum diameter of the knot (d) is reflected by h of the corresponding branch seal (Schulz 1961). The ratio between h and w of a scar seal is directly related to the ratio between the radial extension of the occluded knot (r_1) and the current radius (r_2). This correlation is described by eq. (1) (Schulz 1961).

$$(1) \qquad h/w = r_1/r_2$$

The example in Fig. 4 shows a scar seal quotient of 1:2 and the corresponding longitudinal cut where the ratio between the current radius and the size of the occluded knot is also 1:2. Following this equation, the ratio of a scar seal can be used as a means to predict the share of clear wood for a given log segment.

To validate the correlation between scar seal quotient and knot occlusion, manually assessed branch scars ($n = 1314$) were matched to the corresponding CT-determined knots ($n = 1450$). Therefore, the z position and azimuth of scars and knots were matched. The z position values of the scars were reduced by the height of the Chinese moustache to better match to the z position values of the CT-determined knots. Thresholds of 50 mm and 10° were set for the z position and azimuth, respectively.

Usually hardwood trees do not have a homogenous distribution of knots along the stem. Depending on the position at which the stem is cut to length, logs of different grades can be produced. To test if the simulation of different bucking instructions could be performed by use of t-LiDAR data, each log was virtually segmented into sections of 50 cm in length. For each of these 512 sections, the lowest amount of clear wood as predicted from manually measured branch scars (largest scar seal quotient) and as measured in CT images (largest knot) was calculated.

Figure 6 shows a fictive longitudinal crosscut of a log with several overgrown knots of different sizes. For each 50 cm section, the largest knot determines the amount of clear wood.

Fig. 6. Longitudinal section of a stem separated in sections of 50 cm in length. For each of the sections, the largest knot determines the size of the knotty core (depicted by the broken lines).
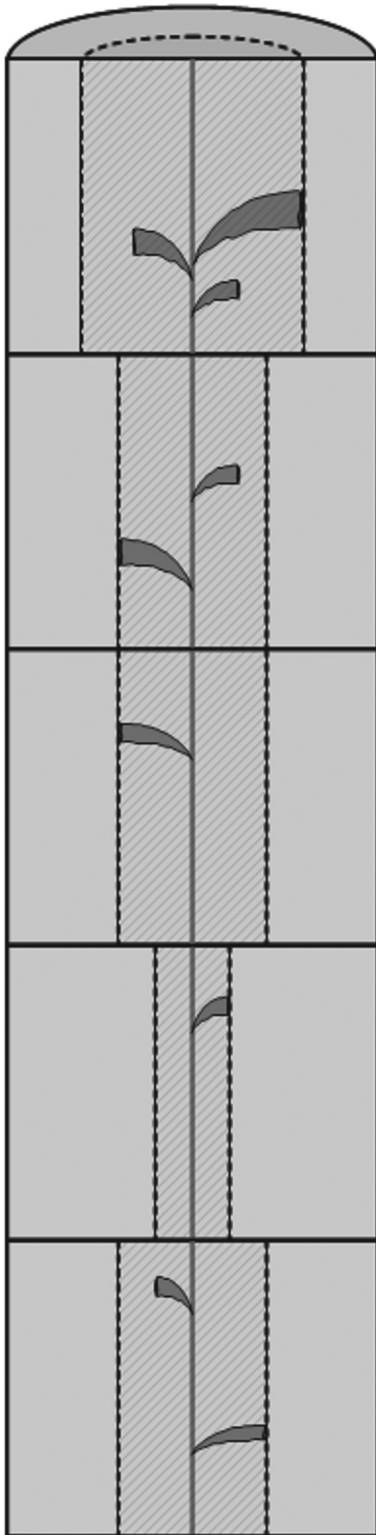
Statistical analysis

Data was analyzed and all statistical tests were performed with the software R (R Development Core Team 2012). The scar seal quotients determined by t-LiDAR and the CT-derived knot lengths were validated with manual measurements. The accuracy was evaluated with "difference versus mean plots" (Bland and Altman 2003), applying the "95% limits of agreement method" suggested by Bland and Altman (1986). The allometric correlations between scar seal size and form and knot size were tested by linear regression analysis. Unrealistic measurements (knotty core larger than 1.2 or scar quotient larger than 1.5) were excluded from the analysis ($n = 2$).

Results

Branch scar assessment with t-LiDAR

Most of the branch scars were assessed directly in the intensity data ($n = 28$). As some of the branch scars could not be identified in the intensity data or the measurement was hard to perform as the edges of the scars seals were difficult to detect, the bark surface model was used for an additional 14 measurements. With both methods, 7 trees had a total of 42 branch scars measured.

Manual validation measurements confirmed the high accuracy of the t-LiDAR measurements at both chosen resolutions. The resolution of 10 000 pixels / 360° was shown to be sufficient and the increase in study site 1 did not enhance the quality of the data. The mean differences of scar height and scar width measured with t-LiDAR compared with manual reference measurements were 5.9 and 8.8 mm, respectively. The relationship between seal height and seal width — the scar seal quotient — of 42 seals was very similar for the t-LiDAR and manual assessment methods (Fig. 7).

Knot measurements with CT

In the CT images, a total of 1450 knots could be identified and measured. Validation measurements on longitudinal cuts showed a high precision for the total knot lengths measured in the CT images (Fig. 8). The absolute maximal error was 19 mm.

Clear wood prediction by applying the scar seal quotient

On the bark surface, 821 branch scars were assessed by manual measurement. Automated matching of knots and branch scars resulted in 666 branch scars that were clearly assignable to knots. One hundred and fifty-five measured branch scars did not originate from overgrown knots but from epicormic shoots or they were caused by bark wounds (false positive). For the remaining 519 knots, no branch scars or only fragmentarily visible scars were found, as they often were too small for detection (false negative).

The correlation between the scar seal quotient and the CT-derived knotty core is shown in Fig. 9. A linear regression analysis of the values from 664 knots confirmed a strong correlation ($R^2 = 0.64$) between scar seal quotient and knotty core. The regression equation $y = 0.86x + 18$ shows a slope that is almost one and an intercept that is close to zero. The root mean square error (RMSE) of 14.59 shows that, on average, the knotty core prediction with the branch scar quotient shows an error of 14.59%. A trend towards overestimating the knotty core by a mean of 10.9% can be observed. This trend does not depend on the extent of the knotty core, but is almost constant. Results also confirmed the finding of Schulz (1961) that the height of the scar seal does strongly correlate with the maximal diameter of the corresponding overgrown knot (Fig. 10).

Results from quality grading of 512 fifty-centimetre sections show that most of the sections (62.5%) were graded identically from their external appearance and the actual knotty core (Table 3). Differing classifications, where the scar assessment underestimated the knotty core, were most often caused by missing branch scars. The most common classification difference (11.5%) was when the branch seal quotient was larger than 1:2 and the knotty core was smaller than 50%.

Fig. 7. Bland–Altman plot of differences between the scar seal quotient derived from the manual assessment and from measurements in terrestrial LiDAR data plotted against the mean of both measurements. The solid line represents the mean difference and the broken lines represent the 95% confidence interval ($n = 42$).
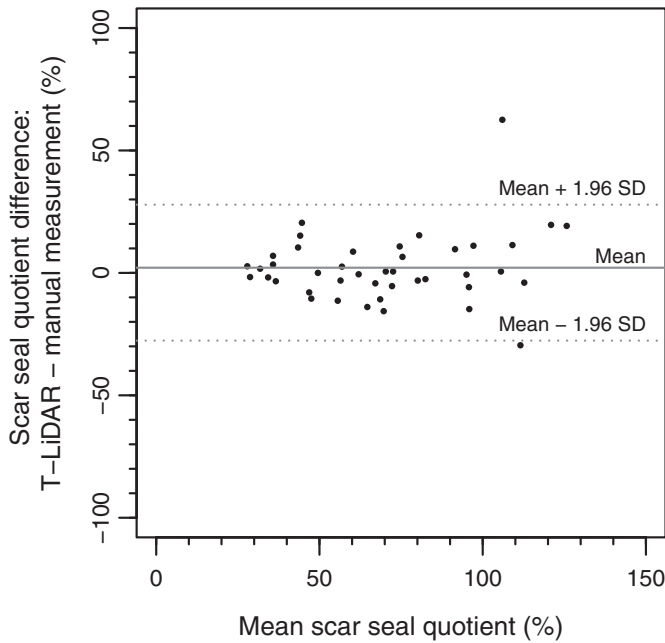

Fig. 8. Bland–Altman plot of differences between the total knot length of 26 knots measured manually on radial cuts and in images from X-ray computed tomography (CT). The solid line represents the mean difference and the broken lines represent the 95% confidence interval.
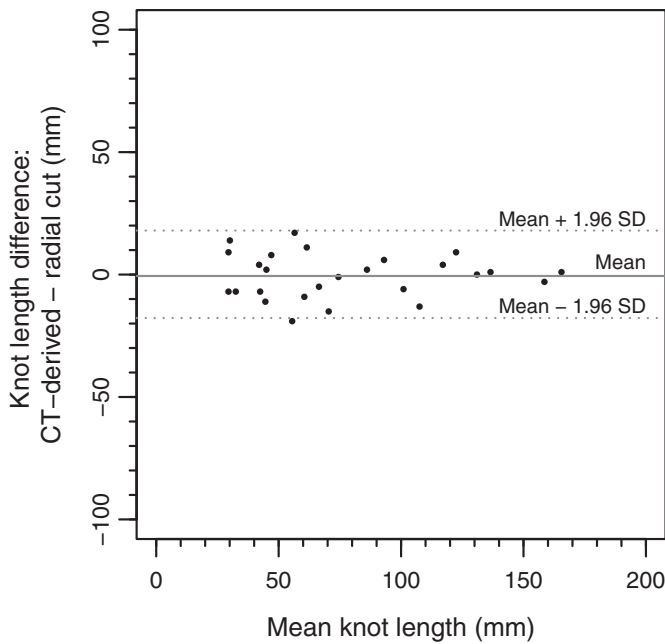

Fig. 9. Calculated knotty core derived from the scar seal quotient versus the computed tomography (CT)-derived knotty core. The regression line is represented by the solid line and the line of equality is represented by the broken line.
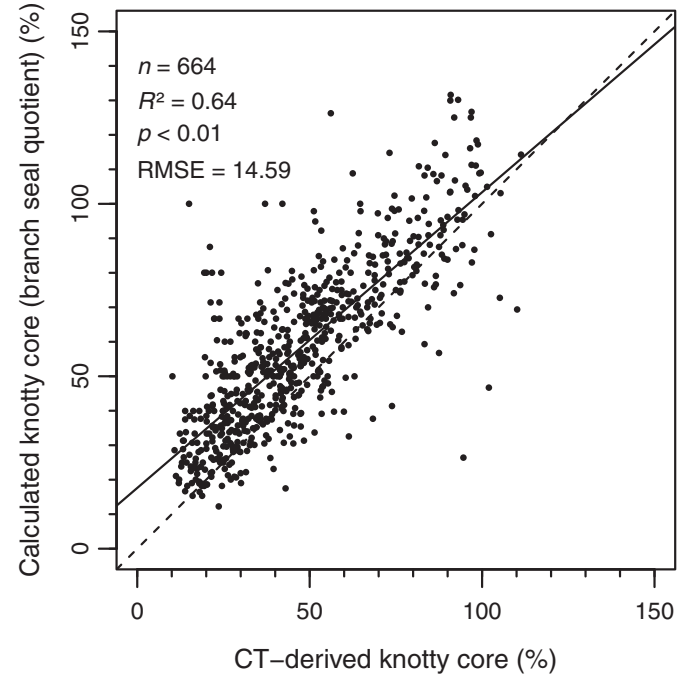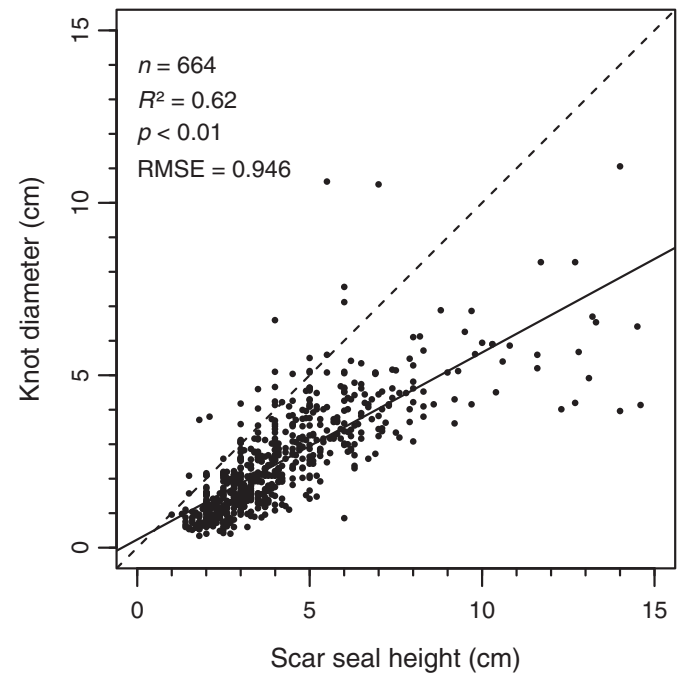

Fig. 10. Maximum computed tomography (CT)-derived knot diameter versus the scar seal height. The regression line is representd by the solid line and the line of equality is represented by the broken line.

Discussion

The results show that t-LiDAR can be used to assess the wood quality of standing beech in more detail by employing the confirmed correlation between scar seal quotient and knotty core (Schulz 1961). This method could be applied to assess the wood quality of several other hardwood species, as many of them also show a correlation between scar seal size and shape and clear wood content (Schulz 1961; Thomas 2009).

The scar seal quotient proved to be reliable when predicting the amount of clear wood for beech. This could be verified for a wide range of knot sizes. The findings support the latest changes in the roundwood grading norm EN 1316-1 (DIN Standard 2013), which

Table 3. Agreement of the quality grading of the 50 cm sections classified by the computed tomography (CT)-derived knotty core with those grades predicted by the scar seal quotient.

Grade quality		Branch scar prediction (%)		
		Grade A	Grade B	Grade C/D
CT	Grade A	7.8	3.5	2.5
	Grade B	8.6*	11.9	11.5
	Grade C/D	6.6*	4.7	42.8
Σ				62.5

Note: Above the diagonal are those segments that were predicted correctly (shaded in gray). Grading was made according to the thresholds for branch seal quotients in EN 1316-1:2012 (DIN Standard 2013).

*Frequently, no scar was visible.

now considers the shape of scar seals for beech roundwood grading.

The correlation between scar seal quotient and knot occlusion is clearly visible; however, high scatter shows that deviation exists (Fig. 9). The largest extent of this deviation can be explained by the natural variation of scar seal shapes. It can also be assumed that measurement errors occurred and branch scars were assigned to knots from which they did not originate.

The number of knots that can be detected in CT images depends heavily on the resolution of the scan, as this determines the minimum size of the visible knots. The high precision of the length measurements of knots shows that precise measurements are possible at the selected scan resolution. It can be assumed, therefore, that all knots, which are important for quality grading, were recognized.

Matching branch scars to the corresponding knots proved to be difficult. For more than half of the knots, it was not possible to define the corresponding bark feature (769 of 1450). Reasons for this difficulty were a high number of knots that were located close to each other, uneven shape of the logs, or spiral grain. Many small knots did not show any bark surface features at all. With knots shorter than 30 mm, only 25% could be matched to a branch scar, whereas 48% of knots longer than 30 mm could be matched with scars.

When analyzing the number of correctly graded virtual segments, it is obvious that not many segments of grade A were found (Table 3). This was due to the low quality of the analyzed trees that showed many branch scars with a seal quotient larger than 1:4, which is the threshold between grades A and B. Further experiments that include more trees of higher quality should be made to evaluate if this approach also can be applied for high-quality wood.

Manual validation measurements of branch scars revealed that scar seal quotients larger than one do occur naturally. Strictly following eq. (1) would lead to a calculated clear wood prediction smaller than zero. The actual measured mean clear wood proportion in all cases with a seal quotient larger than one, however, was 15%. It can be assumed that decisions on bucking instruction or cutting pattern would be the same for a 0% or 15% clear wood prediction; this variation is, therefore, of less importance for practice.

Results show that the accuracy of scar seal measurements with t-LiDAR technology is sufficient to calculate scar seal quotients and, therefore, to deduce information about the position, distribution, and size of the knots. The main difficulty was identifying branch scars in the t-LiDAR data. If the edges of the scars were recognized, the extent of the detail was sufficient to derive reliable scar seal quotients. Terrestrial LiDAR could not be applied to identify branch scars that did not show sufficient distinctiveness in intensity values or radial deviation from the surrounding stem surface. This was true for most of the smaller scars and, therefore, small knots. With increasing height of the tree, it became more difficult to identify and measure branch scars. However, it could

be shown that a combination of the analysis of the intensity data and the bark surface model could be used to assess branch scars up to a height of 7.5 m. This means t-LiDAR could be used as an inventory method for study plots to predict the quality and value of standing trees. This information could then further be used to model the value and future development of stands.

In the CT images of logs, it was hard to discriminate between density differences that are due to wood density and those that are due to moisture content. Nevertheless, we could show for beech that the signal of density difference between the knots and the surrounding wood was strong enough to be recognized. Computed tomography has proven to be useful for the determination of internal wood features such as knots for hardwood species like beech. In practice, CT could be used for the quality grading of logs in sawmills, to improve bucking instructions, and to optimize breakdown in the sawline, if the automated recognition of features and feeding through the scanner work at industrial speed (Giudiceandrea et al. 2011).

The additional information is only worth the effort and cost if the gain from having this information is higher than the costs for getting the information. Before this technology can be used, cost-benefit analysis needs to be performed. Considering the big differences in price for beech timber of different grades, the application of this technology might be economically feasible in forest stands where high-quality beech wood of large diameter can be expected.

Automated knot detection and measurement in CT images already exists for several softwood species (e.g., Grundberg 1999; Oja 2000; Longuetaud et al. 2012). For hardwood species, this should also be automated before implementation in the wood-processing industry can be tested further.

It has already been shown that t-LiDAR can be used to estimate quality criteria such as diameter, length, taper, sweep, crook, and branchiness (Dassot et al. 2011), as well as bark characteristics in the sawmill (Thomas and Thomas 2011) or on site (Schütt et al. 2004). By using the accurate measurement of branch scar seals and the branch scar quotient, one additional quality indicator can be deducted from laser scanning of standing trees: the amount of clear wood, which is of major importance for sawn timber grading.

The accuracy of t-LiDAR for scar measurements is satisfying, but the identification of the scars is difficult. A solution for the development of an automated detection and measurement process could be the use of RGB photos to identify the approximate location of the scars. The Zoller+Fröhlich scanner offers the direct connection to a RGB camera while recording the data to link photos to the 3D scanner data. Together with the intensity values, a better identification might be possible. The measurement of scars using a branch surface model could also be transferred in an automated process, if the approximate location of the scar is known.

Wood quality assessment of standing beech trees with t-LiDAR could be developed by making use of the confirmed correlation between scar seal quotient and the amount of clear wood. Knowledge gained with this technique could provide for better forest planning, improved bucking instructions during harvesting operations, and more precise roundwood grading that could improve the allocation of the roundwood to customers in the industry.

Acknowledgements

editor were very much appreciated and helped improve the manuscript.

References

Anonymous. 2012. Generelle Regeln zur Qualitätssortierung von Stammholz nach der Rahmenvereinbarung für den Rohholzhandel in Deutschland (RVR) [online]. Available from http://www.rvr-deutschland.de/mediapool/61/614960/data/RVR_Sortiertabellen_Laubholz_2012-09-12.pdf [accessed 4 September 2013].

Bland, J.M., and Altman, D.G. 1986. Statistical methods for assessing agreement between two methods of clinical measurement. Lancet, **327**: 307–310. doi:10.1016/S0140-6736(86)90837-8.

Bland, J.M., and Altman, D.G. 2003. Applying the right statistics: analyses of measurement studies. Ultrasound Obstet. Gynecol. **22**(1): 85–93. doi:10.1002/uog.122. PMID:12858311.

Colin, F., Robert, N., Druelle, J.-L., and Fontaine, F. 2008. Initial spacing has little influence on transient epicormic shoots in a 20-year-old sessile oak plantation. Ann. For. Sci. **65**(5): 508. doi:10.1051/forest:2008032.

Curtis, J.D. 1937. An historical review of artificial forest pruning. For. Chron. **13**(2): 380–395. doi:10.5558/tfc13380-2.

Dassot, M., Constant, T., and Fournier, M. 2011. The use of terrestrial LiDAR technology in forest science: application fields, benefits and challenges. Ann. For. Sci. **68**(5): 959–974. doi:10.1007/s13595-011-0102-2.

DIN Standard. 2011. EN 975-1:2009 + AC:2010. Sawn timber — Appearance grading of hardwoods — Part 1: Oak and beech. German version.

DIN Standard. 2013. EN 1316-1:2012. Hardwood round timber — Qualitative classification — Part 1: Oak and beech. German version.

Giudiceandrea, F., Ursella, E., and Vicario, E. 2011. A high speed CT-scanner for the sawmill industry. *In* Proceedings of the 17th International Nondestructive Testing and Evaluation of Wood Symposium, University of West Hungary, Sopron, Hungary, 14–16 September 2011.

Grundberg, S. 1999. An X-ray LogScanner: a tool for control of the sawmill process. Ph.D. thesis, Lulea University of Technology, Skellefteå, Sweden.

Hein, S. 2008. Knot attributes and occlusion of naturally pruned branches of *Fagus sylvatica*. For. Ecol. Manag. **256**(12): 2046–2057. doi:10.1016/j.foreco.2008.07.033.

Hein, S., and Spiecker, H. 2007. Comparative analysis of occluded branch characteristics for *Fraxinus excelsior* and *Acer pseudoplatanus* with natural and artificial pruning. Can. J. For. Res. **37**(8): 1414–1426. doi:10.1139/X06-308.

Knigge, W., and Schulz, H. 1966. Grundriss der Forstbenutzung: Entstehung, Eigenschaften, Verwertung und Verwendung des Holzes und anderer Forstprodukte. Parey, Hamburg, Germany.

Knoke, T., Stang, S., Remler, N., and Seifert, T. 2006. Ranking the importance of quality variables for the price of high quality beech timber (*Fagus sylvatica* L.). Ann. For. Sci. **63**(4): 399–413. doi:10.1051/forest:2006020.

Longuetaud, F., Leban, J.-M., Mothe, F., Kerrien, E., and Berger, M.-O. 2004. Automatic detection of pith on CT images of spruce logs. Comput. Electron. Agric. **44**(2): 107–119. doi:10.1016/j.compag.2004.03.005.

Longuetaud, F., Mothe, F., Kerautret, B., Krähenbühl, A., Hory, L., Leban, J., and Debled-Rennesson, I. 2012. Automatic knot detection and measurements from X-ray CT images of wood: a review and validation of an improved algorithm on softwood samples. Comput. Electron. Agric. **85**: 77–89. doi:10.1016/j.compag.2012.03.013.

Mäkinen, H., and Song, T. 2002. Evaluation of models for branch characteristics of Scots pine in Finland. For. Ecol. Manag. **158**(1): 25–39. doi:10.1016/S0378-1127(00)00672-1.

Mayer-Wegelin, H. 1936. Ästung. Schaper, Hannover, Germany.

Moberg, L., and Nordmark, U. 2006. Predicting lumber volume and grade recovery for Scots pine stems using tree models and sawmill conversion simulation. For. Prod. J. **56**(4): 68–74.

Nicolescu, N.-V. 1999. Artificial pruning-a review. Reprografia Universitatii Transilvania, Brasov, Romania.

O'Hara, K.L. 1989. Forest pruning bibliography. College of Forest Resources, University of Washington.

O'Hara, K.L. 2007. Pruning wounds and occlusion: A long-standing conundrum in forestry. J. For. **105**(3): 131–138.

Oja, J. 2000. Evaluation of knot parameters measured automatically in CT-images of Norway spruce (*Picea abies* (L.) Karst.). Holz als Roh- und Werkstoff, **58**(5): 375–379. doi:10.1007/s001070050448.

Park, J. 1989. Pruned log index. N. Z. J. For. Sci. **19**: 41–53.

Pfeifer, N., and Winterhalder, D. 2004. Modelling of tree cross sections from terrestrial laser-scanning data with free-form curves. *In* Proceedings of the ISPRS Working Group VIII/2: Laser-Scanners for Forest and Landscape Assessment. *Edited by* M. Thies, B. Koch, H. Spiecker, and H. Weinacker. University of Freiburg, Freiburg, Germany. pp. 76–81.

R Development Core Team. 2012. R: A language and environment for statistical computing. Version 2.15.2. R Foundation for Statistical Computing, Vienna, Austria.

Schulz, H. 1961. Die Beurteilung der Qualitätsentwicklung junger Bäume. Forstarchiv, **32**(5): 89–99.

Schütt, C., Aschoff, T., Winterhalder, D., Thies, M., Kretschmer, U., and Spiecker, H. 2004. Approaches for recognition of wood quality of standing trees based on terrestrial laserscanned data. ISPRS, **XXXVI**(8/W2): 179–182.

Storch, J. 2011. Astentwicklung und Astreinigung in Abhängigkeit vom Dickenwachstum bei Buche (*Fagus sylvatica* L.) und Eiche (*Quercus petraea* (Matt.) Liebl.; *Quercus robur* L.). Doctoral Dissertation, Freiburg, Germany.

Thomas, R.E. 2009. Modeling the relationships among internal defect features and external Appalachian hardwood log defect indicators. Silva Fenn. **43**(3): 447–456.

Thomas, L., and Thomas, E.T. 2011. A graphical automated detection system to locate hardwood log surface defects using high-resolution three-dimensional laser scan data. *In* Proceedings of the 17th Central Hardwood Forest Conference; 5–7 April 2010, Lexington, Kentucky. *Edited by* F. Songlin, J.M. Lhotka, J.W. Stringer, K.W. Gottschalk, and G.W. Miller. USDA For. Serv., Northern Research Station, Newtown Square, Penn. Gen. Tech. Rep. NRS-P-78. pp. 92–101.

Van Goethem, G.R.M., van de Kuilen, J.W.G., Gard, W.F., and Ursem, W.N.J. 2008. Quality assessment of standing trees using 3D laserscanning. *In* Proceedings of the Conference in COST E53: Quality Control for Wood and Wood Products. *Edited by* W.F. Gard and J.W.G. van de Kuilen. Delft University of Technology, Delft, The Netherlands. pp. 145–156.

Wei, Q., Leblon, B., and La Rocque, A. 2011. On the use of X-ray computed tomography for determining wood properties: a review. Can. J. For. Res. **41**(11): 2120–2140. doi:10.1139/x11-111.

Wernsdörfer, H., Le Moguédec, G., Constant, T., Mothe, F., Nepveu, G., and Seeling, U. 2006. Modelling of the shape of red heartwood in beech trees (*Fagus sylvatica* L.) based on external tree characteristics. Ann. For. Sci. **63**(8): 905–913. doi:10.1051/forest:2006074.